UPPER LEVEL BAROTROPIC INSTABILITY IN THE TROPICS

Ronnie J. Hartinger

NAVAL POSTGRADUATE SCHOOL
Monterey, California

THESIS

UPPER LEVEL BAROTROPIC INSTABILITY

by

Ronnie J. Hartinger

September 1975

Thesis Advisor: R. T. Williams

Approved for public release; distribution unlimited.

Unclassified

SECURITY CLASSIFICATION OF THIS PAGE (When Data Entered)

REPORT DOCUMENTATION PAGE		READ INSTRUCTIONS BEFORE COMPLETING FORM
1. REPORT NUMBER	2. GOVT ACCESSION NO.	3. RECIPIENT'S CATALOG NUMBER
4. TITLE (and Subtitle) Upper Level Barotropic Instability in the Tropics		5. TYPE OF REPORT & PERIOD COVERED Master's Thesis; September 1975 6. PERFORMING ORG. REPORT NUMBER
7. AUTHOR(s) Ronnie J. Hartinger		8. CONTRACT OR GRANT NUMBER(s)
9. PERFORMING ORGANIZATION NAME AND ADDRESS Naval Postgraduate School Monterey, California 93940		10. PROGRAM ELEMENT, PROJECT, TASK AREA & WORK UNIT NUMBERS
11. CONTROLLING OFFICE NAME AND ADDRESS Naval Postgraduate School Monterey, California 93940		12. REPORT DATE September 1975 13. NUMBER OF PAGES 40
14. MONITORING AGENCY NAME & ADDRESS(if different from Controlling Office) Naval Postgraduate School Monterey, California 93940		15. SECURITY CLASS. (of this report) Unclassified 15a. DECLASSIFICATION/DOWNGRADING SCHEDULE

16. DISTRIBUTION STATEMENT (of this Report)

Approved for public release; distribution unlimited.

17. DISTRIBUTION STATEMENT (of the abstract entered in Block 20, if different from Report)

18. SUPPLEMENTARY NOTES

19. KEY WORDS (Continue on reverse side if necessary and identify by block number)

Barotropic instability
CISK heating
Two-level model
Growth rates of easterly flow

20. ABSTRACT (Continue on reverse side if necessary and identify by block number)

The structure of barotropically unstable disturbances in the tropics was examined with a two-level quasi-geostrophic model. The forecast equations were linearized and non-dimensionalized and the most unstable mode was found numerically by use of the initial value technique. The wind profile $U_j = a_j U_o \operatorname{sech}^2(y/L)$ was used. Simple CISK type heating was introduced to determine its effects on the growth

DD FORM 1 JAN 73 1473 (Page 1)

EDITION OF 1 NOV 65 IS OBSOLETE

S/N 0102-014-6601 |

Unclassified

SECURITY CLASSIFICATION OF THIS PAGE (When Data Entered)

of the waves. The jet wind profile was more unstable with easterly flow than westerly flow when no heating or friction was present. When the jet profile was present only at the upper level, the ratio of the disturbance amplitude at the lower level to the disturbance amplitude at the upper level decreased toward the equator. When the heating rate was not large enough to increase the growth rate, the amplitude ratio remained small. As the heating rate becomes larger, the ratio increases to a value larger than 1.

Upper Level Barotropic Instability in the Tropics

by

Ronnie J. Hartinger
Lieutenant Commander, United States Navy
B.S., San Jose State College, 1963

Submitted in partial fulfillment of the requirements for the degree of

MASTER OF SCIENCE IN METEOROLOGY

from the

NAVAL POSTGRADUATE SCHOOL

September 1975

ABSTRACT

The structure of barotropically unstable disturbances in the tropics was examined with a two-level quasi-geostrophic model. The forecast equations were linearized and non-dimensionalized and the most unstable mode was found numerically by use of the initial value technique. The wind profile $U_j = a_j U_o \mathrm{sech}^2(y/L)$ was used. Simple CISK type heating was introduced to determine its effects on the growth of the waves. The jet wind profile was more unstable with easterly flow than westerly flow when no heating or friction was present. When the jet profile was present only at the upper level, the ratio of the disturbance amplitude at the lower level to the disturbance amplitude at the upper level decreased toward the equator. When the heating rate was not large enough to increase the growth rate, the amplitude ratio remained small. As the heating rate becomes larger, the ratio increases to a value larger than 1.

TABLE OF CONTENTS

I. INTRODUCTION---------- 8

II. THE FORECAST EQUATIONS----------10

III. BOUNDARY CONDITIONS AND FINITE DIFFERENCING SCHEME----------17

IV. WIND PROFILES AND INITIAL CONDITIONS----------19

V. NON-DIMENSIONALIZATION PROCEDURE----------20

VI. COMPUTATIONAL PROCEDURE----------22

VII. RESULTS----------24

VIII. CONCLUSIONS----------33

LIST OF REFERENCES----------35

INITIAL DISTRIBUTION LIST----------38

TABLE OF SYMBOLS & ABBREVIATIONS

A_e	Vertical eddy viscosity
β_o	Derivative of corcolis parameter at y = 0
C_p	Specific heat at constant pressure
f_o	Coriolis parameter at y = 0
g	Gravity
ω	dp/dt
Ψ	gz/f_o
R	Gas constant for dry air
ρ	Density
T_s	Average temperature from the standard atmosphere
σ	$(R^2T_s/p^2g)(\partial T_s/\partial z + g/C_p)$
ζ	$\nabla^2\Psi$
z	Height
Q	Heating added per unit mass
∇^4	Bi-harmonic operator $(\nabla^2)^2$
α	Wind inflow angle

ACKNOWLEDGEMENT

The author wishes to express his deep appreciation to Dr. Roger Terry Williams for his understanding, guidance, and encouragement in the preparation of this thesis and to Dr. C. P. Chang for his useful comments. A sincere thank you to T. G. Robertson who allowed his model to be modified for the experiments conducted. In addition, to thank my wife Vicki, whose quiet understanding and patience made this effort possible.

I. INTRODUCTION

In the last few years there has been growing evidence that barotropic instability may be a common occurrence at the 200-mb level in the tropics. Krishnamurti [1970, 1971] observed a peak at wave numbers 6-8 in the wind spectrum at this level which he proposed was caused by barotropic instability. A subsequent study by Kanamitsu, et al. [1972] showed that for the region between 15S and 15N waves of this scale do receive energy through barotropic interaction with the zonal mean flow and zonal wave number 1.

Kuo [1949] examined the barotropic stability characteristics of a parallel zonal current and found that instability is possible only if the gradient of the absolute vorticity changes sign somewhere in the region. The 200-mb level in the tropics is the outflow level of the giant monsoon circulation which is induced by differential heating (both sensible and latent) due to land-sea distribution. The basic flow pattern thus varies in the planetary scale. Detailed observations have found that synoptic-scale moving disturbances at this level tend to form in the easterly jet south of the Tibetan high [Krishnamurti, 1970] during the northern hemisphere summer. This is a region of large vorticity gradient where the necessary condition for instability is occasionally satisfied locally. If these waves were the result of barotropic instability, they would extract energy from the mean

flow and the long waves, since the long waves and the mean flow combine to give large vorticity gradients in these regions. The energy exchanges computed by Kanamitsu et al. [1972] are consistent with this view.

In this thesis the barotropic instability of an upper level easterly jet was examined. In addition to the calculation of the growth rates, the downward propagation of energy was also investigated to examine the possibility that lower troposphere tropical disturbances may originate at the upper levels. Simple CISK type heating was introduced to ascertain how it affects the growth of the waves.

This study uses a quasi-geostrophic two-level model. The equations are linearized and solved by the initial value technique. Growth rate and wave structure are extracted after an exponential growth is established.

II. THE FORECAST EQUATIONS

The quasi-geostrophic prediction equations were used as the forecast equations. It is recognized that the quasi-geostrophic approximation is not very accurate near the Equator, but Matsuno [1966] has shown with a barotropic model that quasi-geostrophic motions are identifiable near the Equator if the wavelength is not too long. Also, in a study with a baroclinic model, Yamasaki [1969] has found that the error is small at twenty degrees latitude.

The quasi-geostrophic equations are simplified through the use of a two-level model. The basic model is very similar to the models used by Williams et al. [1971] and Robertson [1973]. The equations were linearized and solved numerically by the initial value technique. The growth rates and wave structures were then computed.

The simple two-level model was constructed by dividing the atmosphere into four layers with a constant pressure differential of $\Delta p/2$ (Fig. 1), numbered 0 to 4 from top to bottom. The boundary condition at $p = p_t$ was $\omega_o = 0$, which prohibits vertical propagation of energy. Charney [1969] has shown that such energy propagation is unlikely. At $p = p_o$ the boundary condition was $\omega = \omega_e$ where ω_e was the frictionally induced ω at the top of the Ekman layer. Charney and Eliassen [1949] derived the following expression for ω_e.

$$\omega_e = -\rho_4 g \left(\frac{A_e}{2f_o}\right)^{1/2} \sin 2\alpha \, \zeta_4 \qquad (2.1)$$

where A_e is the kinematic eddy viscosity, α is the surface inflow angle, and ζ_4 is the surface geostrophic vorticity.

p		Level
p_t	$\omega_o = 0$	0
	Ψ_1	1
$p_t + \Delta p$	ω_2	2
	Ψ_3	3
p_o	$\omega = \omega_e$	4

Fig. 1. Two-level prediction model

It has been shown by Holton et al. [1971] and Chang [1973] that this expression is reasonably valid as far equatorward as ten degrees, but may be invalid close to the Equator south of the ITCZ. The surface geostrophic vorticity was approximated by

$$\zeta_4 \simeq \zeta_3 = \nabla^2 \Psi_3 \qquad (2.2)$$

The quasi-geostrophic vorticity equation in pressure coordinates is

$$\frac{\partial}{\partial t}\nabla^2\Psi + |K \times \nabla\Psi \cdot \nabla(\nabla^2\Psi) + \beta_o \frac{\partial \Psi}{\partial x} - f_o \frac{\partial \omega}{\partial p} = 0 \qquad (2.3)$$

where $f_o = 2\Omega \sin \psi_o$, $\beta_o = 2\Omega \cos \psi_o / a$, $\omega = dp/dt$, Ψ = stream function, ψ_o is the reference latitude, and a is the radius of the earth. Observe that when $\omega = 0$, (2.3) becomes the

barotropic vorticity equation which is sufficient to describe the barotropic instability.

Applying this equation at levels 1 and 3 gives

$$\frac{\partial}{\partial t}\nabla^2\Psi_1 + \not{K} \times \nabla\Psi_1 \cdot \nabla(\nabla^2\Psi_1) + \beta_o \frac{\partial\Psi_1}{\partial x} - f_o \frac{\omega_2}{\Delta p} = 0, \qquad (2.4)$$

$$\frac{\partial}{\partial t}\nabla^2\Psi_3 + \not{K} \times \nabla\Psi_3 \cdot \nabla(\nabla^2\Psi_3) + \beta_o \frac{\partial\Psi_3}{\partial x} - f_o \frac{(\omega_4 - \omega_2)}{\Delta p} = 0. \qquad (2.5)$$

If it is desired to stop at some intermediate point, say the tropopause, rather than to include the entire atmosphere, smaller layers could be used.

Next, consider the quasi-geostrophic first law of thermodynamics in the form

$$\frac{\partial}{\partial t}\frac{\partial\Psi}{\partial p} + \not{K} \times \nabla\Psi \cdot \nabla\left(\frac{\partial\Psi}{\partial p}\right) + \frac{\sigma}{f_o}\omega = 0 \qquad (2.6)$$

where

$$\sigma = \frac{R^2 T_s}{p^2 g}\left[\frac{dT_s}{dz} + \frac{g}{C_p}\right], \qquad (2.6a)$$

and T_s is the temperature obtained from the standard atmosphere.

The heating follows the formulation of Ooyama [1964], Charney and Eliassen [1964], and Kuo [1965], i.e., the condensation heating is proportional to the convergence of moisture in the Ekman layer. The form used was given by Ogura [1964]:

$$Q_2 = \frac{1}{2}\frac{C_p T_s}{\bar{\theta}}\frac{\partial\bar{\theta}}{\partial p}\eta\omega_4 \qquad (2.7)$$

where η is a non-dimensional parameter. This relationship was used in both rising and subsiding air representing a Fourier expansion

of the heating function. The factor 1/2 is therefore needed to maintain the correct amplitude of the heating perturbation.

When (2.6) is appled at level 2 the result is

$$\frac{\partial}{\partial t}(\Psi_1 - \Psi_3) + |K \times \nabla(\frac{\Psi_1 + \Psi_3}{2}) \cdot \nabla(\Psi_1 - \Psi_3) - \frac{\Delta p \sigma_2 \omega_2}{f_o} = 0. \quad (2.8)$$

Define the following quantities

$$\Psi_M = \frac{\Psi_1 + \Psi_3}{2}, \quad (2.9)$$

$$\Psi_T = \frac{\Psi_1 - \Psi_3}{2}, \quad (2.10)$$

which implies that

$$\Psi_1 = \Psi_M + \Psi_T, \quad (2.11)$$

$$\Psi_3 = \Psi_M - \Psi_T. \quad (2.12)$$

Here Ψ_T is proportional to the layer thickness and is therefore a measure of the mean temperature in the layer. Using these definitions, add (2.4) and (2.5) and divide the result by two, obtaining

$$\frac{\partial}{\partial t}\nabla^2\Psi_M + |K \times \nabla\Psi_M \cdot \nabla(\nabla^2\Psi_M) + |K \times \nabla\Psi_T \cdot \nabla(\nabla^2\Psi_T)$$

$$+ \beta_o \frac{\partial \Psi_M}{\partial x} - \frac{f_o \omega_e}{2\Delta p} = 0 \quad (2.13)$$

For the second forecast equation, subtract (2.5) from (2.4) and eliminate ω_2 by using (2.8) obtaining

$$\frac{\partial}{\partial t}(\nabla^2 - \mu^2)\,\Psi_T + |K \times \nabla\Psi_M \cdot \nabla(\nabla^2 - \mu^2)\Psi_T + |K \times \nabla\Psi_T \cdot \nabla(\nabla^2\Psi_M)$$

$$+ \beta_o \frac{\partial \Psi_T}{\partial x} + \frac{f_o \omega_e}{2\Delta p} = 0, \qquad (2.14)$$

where

$$\mu^2 = \frac{2f_o^2}{\Delta p^2 \sigma_2} \,. \qquad (2.14a)$$

These are the prediction equations for the model.

Although the normal mode method gives the phase speeds, growth rates, and wave structures for all modes, the initial value approach gives the phase speed, growth rate, and wave structure of only the most unstable mode. This approach was chosen because only information about the most unstable mode was needed.

It is convenient to write ψ_M and ψ_T in the following form:

$$\psi_M = E(y) + A(y,t) \cos kx + B(y,t) \sin kx, \qquad (2.15)$$

$$\psi_T = F(y) + C(y,t) \cos kx + D(y,t) \sin kx. \qquad (2.16)$$

where k is the x wave number. The coefficients A through D are the Fourier amplitudes of the disturbance and E and F are the mean zonal fields.

These expressions for ψ_M and ψ_T are substituted into (2.13). The various sine and cosine terms are then separated, and all products of the quantities A through D neglected. Equating the coefficients of the cosine terms gives

$$\frac{\partial}{\partial t}\left(\frac{\partial^2 A}{\partial y^2} - Ak^2\right) = k\left[\frac{\partial E}{\partial y}\frac{\partial^2 B}{\partial y^2} + \frac{\partial F}{\partial y}\frac{\partial^2 D}{\partial y^2} - \frac{\partial^3 E}{\partial y^3}B - \frac{\partial^3 F}{\partial y^3}D\right.$$

$$\left. - k^2\left(\frac{\partial E}{\partial y}B + \frac{\partial F}{\partial y}D\right)\right] - \beta_o Bk - K\left(\frac{\partial^2}{\partial y^2} - k^2\right)(A - C). \tag{2.17}$$

For the sine terms the result is

$$\frac{\partial}{\partial t}\left(\frac{\partial^2 B}{\partial y^2} - Bk^2\right) = k\left[-\frac{\partial E}{\partial y}\frac{\partial^2 A}{\partial y^2} - \frac{\partial F}{\partial y}\frac{\partial^2 C}{\partial y^2} + \frac{\partial^3 E}{\partial y^3}A + \frac{\partial^3 F}{\partial y^3}C\right.$$

$$\left. + k^2\left(\frac{\partial E}{\partial y}A + \frac{\partial F}{\partial y}C\right)\right] + \beta_o Ak - K\left(\frac{\partial^2}{\partial y^2} - k^2\right)(B - D). \tag{2.18}$$

Repeat the procedure for equation (2.14) for the cosine terms which gives

$$\frac{\partial}{\partial t}\left(\frac{\partial^2 C}{\partial y^2} - Ck^2 - C\mu^2\right) = k\left[\frac{\partial E}{\partial y}\frac{\partial^2 D}{\partial y^2} + \frac{\partial F}{\partial y}\frac{\partial^2 B}{\partial y^2} - \frac{\partial E}{\partial y}D\left(k^2 + \mu^2\right)\right.$$

$$\left. - \frac{\partial F}{\partial y}B\left(k^2 - \mu^2\right) - \frac{\partial^3 E}{\partial y^3}D - \frac{\partial^3 F}{\partial y^3}B\right]$$

$$- \beta_o Dk + (K - S)\left(\frac{\partial^2}{\partial y^2} - k^2\right)(A - C). \tag{2.19}$$

The results for the sine terms are

$$\frac{\partial}{\partial t}\left(\frac{\partial^2 D}{\partial y^2} - Dk^2 - D\mu^2\right) = k\left[\frac{\partial E}{\partial y}C\left(k^2 + \mu^2\right) + \frac{\partial F}{\partial y}A\left(k^2 - \mu^2\right)\right.$$

$$\left. - \frac{\partial E}{\partial y}\frac{\partial^2 C}{\partial y^2} - \frac{\partial F}{\partial y}\frac{\partial^2 A}{\partial y^2} + \frac{\partial^3 F}{\partial y^3}A + \frac{\partial^3 E}{\partial y^3}C\right]$$

$$+ \beta_o Ck + (K - S)\left(\frac{\partial^2}{\partial y^2} - k^2\right)(B - D), \tag{2.20}$$

where

$$K = \frac{f_o g}{2RT_s}\left(\frac{\Lambda_M}{f_o}\right)^{1/2} \tag{2.20a}$$

and

$$S = \frac{g}{8} \frac{\eta}{|\theta|} \frac{\partial \bar{\theta}}{\partial p} \frac{p_o}{f_o} \left(\frac{A_M}{f_o}\right)^{1/2} . \tag{2.21}$$

The computational equation for vertical velocity is given below:

$$\omega_2 = \frac{2}{\Delta p \sigma} \left[\frac{\partial \psi_T}{\partial t} + u_m \frac{\partial \psi_T}{\partial x} + v_m \frac{\partial \psi_T}{\partial y} + \frac{KQ_z}{2f_o}\right], \tag{2.22}$$

where

$$u_m = - \frac{1}{f_o} \frac{\partial \psi_M}{\partial y} , \tag{2.23}$$

$$v_m = \frac{1}{f_o} \frac{\partial \psi_M}{\partial x} . \tag{2.24}$$

III. BOUNDARY CONDITIONS AND FINITE DIFFERENCING SCHEME

The finite difference scheme is illustrated below with a sample variable M:

$$\frac{\partial M}{\partial y} = \frac{1}{2H} (M_{i+1} - M_{i-1}) , \tag{3.1}$$

$$\frac{\partial^2 M}{\partial y^2} = \frac{1}{H^2} (M_{i+1} - 2M_i + M_{i-1}) , \tag{3.2}$$

$$\frac{\partial^3 M}{\partial y^3} = \frac{1}{2H^3} [(M_{i+2} - 2M_{i+1} + M_i) - (M_i - 2M_{i-1} + M_{i-2})] \tag{3.3}$$

where i is the grid index and H is the distance between grid points.

Centered time differences were used for all quantities except those involving friction and heating. The friction and heating terms were computed at time $(t - \Delta t)$. The first step in all cases is a forward time step. The second order equations for time tendencies were solved by the exact method of Richtmyer [1957, p. 101].

Yanai and Nitta [1968a] studied the problem of using finite difference equations to solve dynamic instability problems of non-divergent barotropic currents with boundaries. In this study rigid boundaries are placed at $y = \pm W/2$ where W is the total width of the computational field. The boundary conditions were $A = B = C = D = 0$ at $y = \pm W/2$.

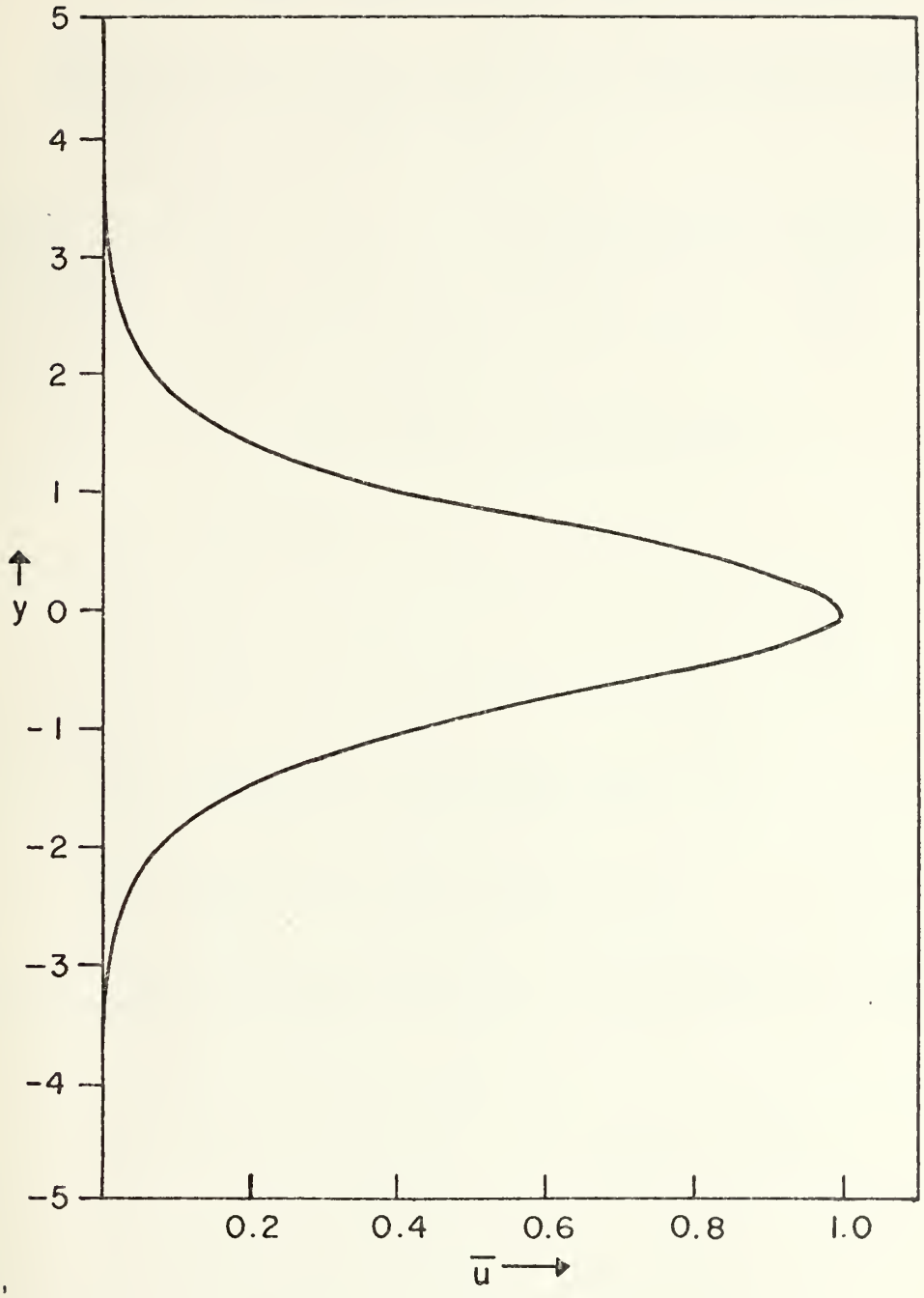

Fig. 2. Mean wind profile $U_j = a_j U_o \text{ sech}^2 (y/L)$

IV. WIND PROFILE AND INITIAL CONDITIONS

This study uses the following zonal wind profile:

$$U_j = a_j U_o \operatorname{sech}^2 (y/L), \tag{4.1}$$

where a_j can be ± 1 or 0. The barotropic stability of this profile has been analyzed by Lipps [1962]. Figure 2 contains the profile (4.1) for $a_j = 1$.

The initial conditions are given below:

$$A = \sin \pi y/W \tag{4.2}$$

$$B = 0 \tag{4.3}$$

$$C = 0 \tag{4.4}$$

$$D = 0 \tag{4.5}$$

$$E = \frac{a_1 + a_3}{2} f_o U_o L \tanh (y/L) \tag{4.6}$$

$$F = \frac{a_1 - a_3}{2} f_o U_o L \tanh (y/L) \tag{4.7}$$

Note that the E and F fields are independent of time.

V. NON-DIMENSIONALIZATION PROCEDURE

In order to simplify the interpretation of the results, the equations are written in non-dimensional form as follows: $x = Lx'$, $y = Ly'$, and $t = L/t'$. The stream function is written

$$\Psi_M = - LU_o \int \bar{u}_M (y')dy' + \psi_M(x',y',t') \tag{5.1}$$

and

$$\Psi_T = - LU_o \int \bar{u}_T (y')dy' + \psi_T(x',y',t') \tag{5.2}$$

when these expressions are substituted into (2.13) and (2.14), and when the products of the ψ's are dropped, the non-dimensional equations can be written:

$$(\frac{\partial}{\partial t} + \bar{u}\frac{\partial}{\partial x})\nabla^2\psi_M + (\hat{\beta} - \frac{d^2\bar{u}}{dy^2})\frac{\partial \psi_M}{\partial x} + \Gamma\nabla^2(\psi_M - \psi_T) = 0 \tag{5.3}$$

$$(\frac{\partial}{\partial t} + \bar{u}\frac{\partial}{\partial x})(\nabla^2 - \varepsilon)\psi_T + (\hat{\beta} - \frac{d^2\bar{u}}{dy^2})\frac{\partial \psi_T}{\partial x} + (\delta - \Gamma)\nabla^2(\psi_M - \psi_T) = 0 \tag{5.4}$$

where

$$\varepsilon = L^2\mu^2, \quad \hat{\beta} = \beta_o L^2 U^{-1}, \quad \Gamma = \frac{f_o L}{U}\frac{\sin 2\alpha}{2\Delta p/\rho_4 g}(\frac{A_e}{2f_o})^{1/2} \tag{5.5}$$

and

$$\delta = \frac{\eta \max\ L\ p_o\ g\ \mu^2 |\frac{\partial \theta}{\partial p}| \sin 2\alpha}{U_o 4\ f_o\ T_4}(\frac{A_e}{2f_o})^{1/2} \tag{5.6}$$

The quantity ε is a rotational Froude number, $\hat{\beta}$ is a non-dimensional form of β, Γ is the ratio of the square root of the Ekman number [Greenspan, 1968] to the Rossby number, and

δ is the heating parameter. The primes on the independent variables have been dropped. These equations are equivalent to the set 2.17, 2.18, 2.19, and 2.20 which were solved numerically.

VI. COMPUTATIONAL PROCEDURE

The following constants were used in the computations:

p_o = 100 centibars,

L = 400 kilometers,

W = 4000 kilometers,

U_o = 10 meters per second,

f_o = varied with latitude,

σ = 3.0 meters per second squared per centibar squared,

β = varied with latitude,

Δp = 50 centibars,

A_e = 10 meters per second squared,

α = 22.5 degrees,

μ^2 = varied with latitude

H = 50 kilometers,

Δt = 1.0 hours,

η_{max} = 4, 6, 8

$\partial\bar{\theta}/\partial p$ = -0.6 degrees per centibar.

A forecast period of 100 days was used so that the most unstable mode would have reached the maximum growth rate. For convenience, growth rates were computed over the last two days of the forecast period. This was done by assuming the amplitudes could be written as

$$x_1 = a_o \exp (n U_o/L) t_1, \quad (6.1)$$

$$x_2 = a_o \exp (n U_o/L) t_2, \quad (6.2)$$

where n is the non-dimensional growth rate and a_o is a constant. By forming the ratio x_2/x_1, the growth rate can be shown to be

$$n = \frac{L \ln (x_2/x_1)}{U_o (t_2 - t_1)} . \qquad (6.3)$$

VII. RESULTS

A series of experiments were conducted over a wide variety of conditions. The more important experiments are given in Table I as a function of a_1, a_3, $\hat{\beta}$, ε, δ, Γ, n, and k′, where n represents the maximum growth rate for each set of conditions and k′ is the corresponding non-dimensional wave number kL. When some of these parameters were computed over a range of values, the range is given.

Experiment 1 was conducted to determine the difference in growth rate characteristics between easterly and westerly jets. In this experiment no heating or friction was included and the mean flow was the same at both levels. In order to obtain a continuous variation between the easterly and westerly flows, the non-dimensional parameter $\hat{\beta}$ (see equation 5.5) was defined to assume the sign of U. Thus $\hat{\beta}$ is positive for westerly flow and negative for easterly flow. In the remaining experiments the jet will be easterly, but $\hat{\beta}$ will be regarded as positive. For each $\hat{\beta}$ the maximum growth rate and the corresponding wave number were determined. Figure 3 contains these quantities as a function of $\hat{\beta}$; the maximum growth rate of n = 0.1888 and occurs at $\hat{\beta}$ = -0.352. The corresponding wave number is k′ = 0.99. This value of k′ is close to the minimum k′ which occurs when $\hat{\beta}$ = -0.112. Fig. 3 shows clearly that the easterly jet is more unstable than the westerly jet. In particular, the growth rates for the easterlies over a range of beta are

greater than the value for beta = 0. This is in contrast to the normal notion that the presence of beta has a stabilizing effect for instabilities.

Experiment 2 investigated the downward propagation of energy from a barotropically unstable disturbance as a function of the latitudinal location of the jet. An easterly jet was introduced at the upper level and the lower level mean flow was set to zero. Surface friction was included, but heating was neglected. A measure of the downward propagation is the ratio $R = |\Psi_3|_{max}/|\Psi_1|_{max}$ where these amplitudes are obtained from the exponentially unstable solution. Figure 4 contains isolines of R as a function of k' and latitude. The curve n_{max} shows the wave number which has the maximum growth rate at each latitude. The R value decreases as one moves from high to low latitude as predicted by Charney [1963]. The R value also decreases with increasing wave number at each latitude. This figure shows the dependence on epsilon.

Experiments 3, 4, and 5 all contain heating and were conducted with a fixed latitude of 10 degrees, otherwise they are the same as experiment 2. In these experiments a weighting factor was applied to the heating following Bates [1970] and Yamasaki and Wada [1972]. The following expression was used

$$\eta = \eta_{max}/\cosh^2 y/L. \qquad (7.1)$$

This form implies that moisture is available for the heating in the region $|y| \lesssim L$. If this was not done, CISK heating would occur in regions away from the basic jet. In experiment 3

where $\eta_{max} = 4$ the non-dimensional heating parameter is $\delta = 0.165$. Figure 5 shows the growth rate (n) and the amplitude ratio (R) as a function of the non-dimensional wave number k'. Note that the maximum growth rate of n = 0.187 occurs at $k' = 1.0$. These two values are very close to the values obtained without heating. The R is fairly large at the lower values of k' with a maximum at 0.5. R becomes very small in the area of maximum growth. Apparently the barotropic instability effects dominate in the areas of maximum growth while the heating is relatively more important for $k' \leq 0.5$ as evidenced by the larger values of R. This effect is even more pronounced in experiment 4.

In experiment 4 where $\eta_{max} = 6$ the non-dimensional heating parameter is $\delta = 0.247$. Figure 6 shows that the maximum growth rate of n = 0.186 occurs at $k' = 1.0$ just as in experiment 3. As k' varies away from 1.0 to either extreme the growth rate approaches 0.167. The R is larger in both of these regions where the largest value occurs for the largest value of k'. A secondary maximum in R occurs at $k' = 0.6$. This indicates that heating dominates the solution in the regions which have the larger values of R.

In experiment 5 where $\eta_{max} = 8$ the non-dimensional heating parameter is $\delta = 0.330$. Figure 7 shows that the growth rate is fairly constant over the k' considered. This is similar to the results obtained by Williams and Robertson [1973] who acquired essentially a constant growth rate with a hyperbolic tangent wind profile using larger values of δ.

Experiment	a_1	a_3	$\hat{\beta}$	k'	δ	Γ	n	ε
1	1	1	-1.536 to 0.448	0.9	0	0.0	0.189	0.106
2	-1	0	0.182 to 0.360	1.0	0	0.036 to 0.840	0.188	0.027 to 0.677
3	-1	0	0.36	1.0	0.165	0.036	0.187	0.027
4	-1	0	0.36	1.0	0.247	0.036	0.186	0.027
5	-1	0	0.36	--	0.330	0.036	0.247	0.027

TABLE I

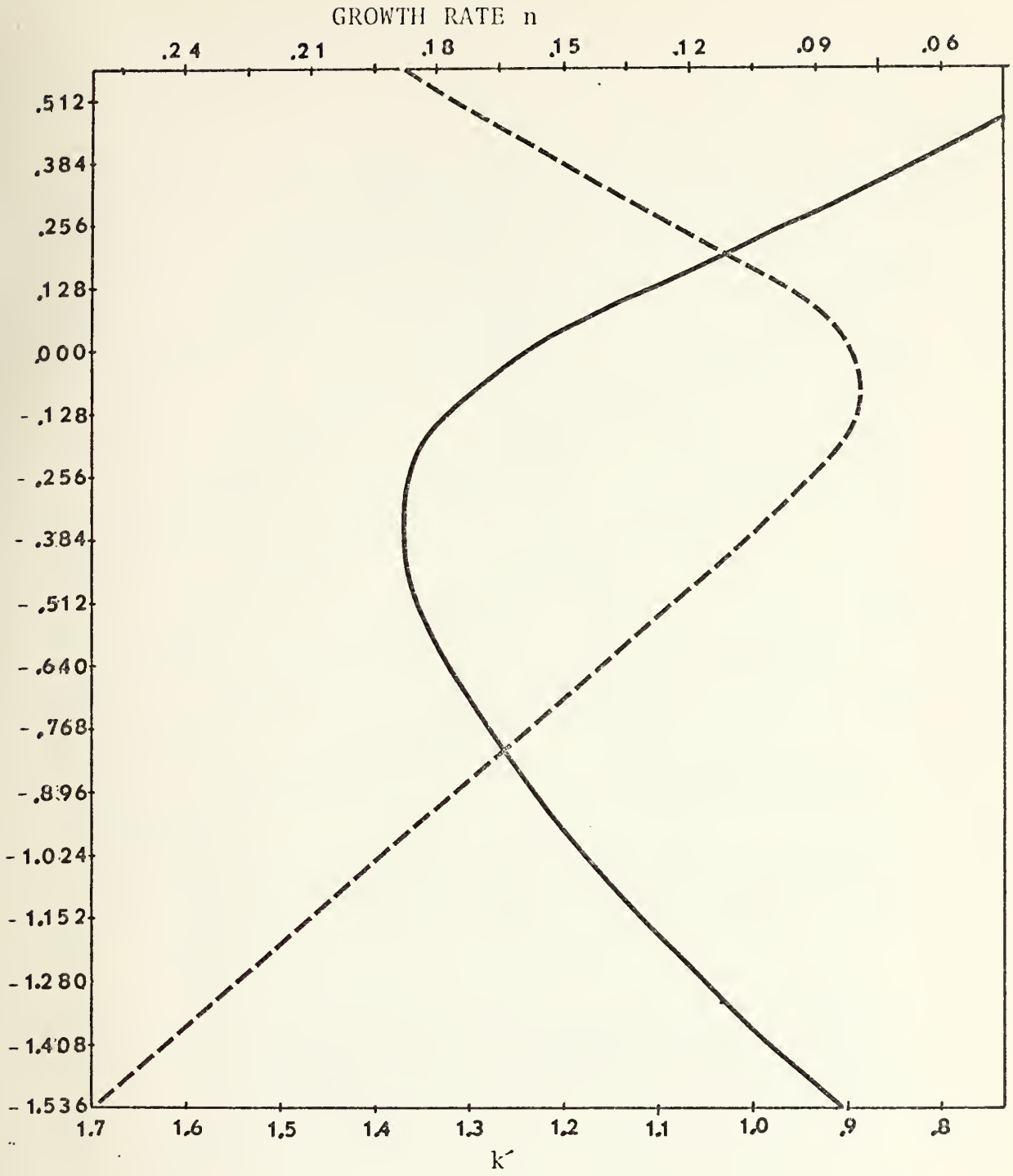

Fig. 5. The growth rate n (solid line) and the corresponding wave number k´(dashed line) as functions of $\hat{\beta}$ for experiment 1. Westerly flow occurs for $\hat{\beta} > 0$ and easterly flow for $\hat{\beta} < 0$.

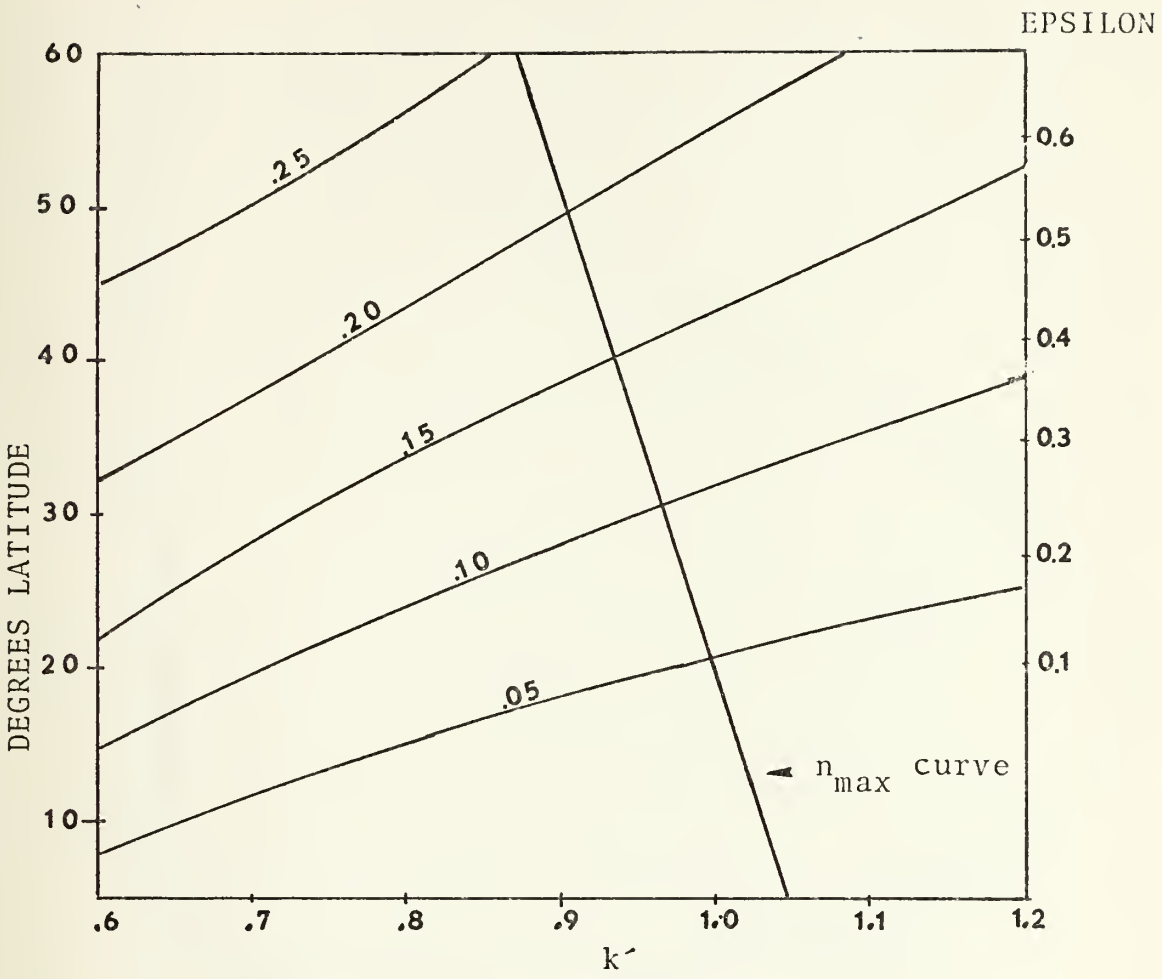

Fig. 4. Isolines of $R = |\Psi_3|_{max}/|\Psi_1|_{max}$ (curved lines) as functions of k´, latitude, and epsilon.

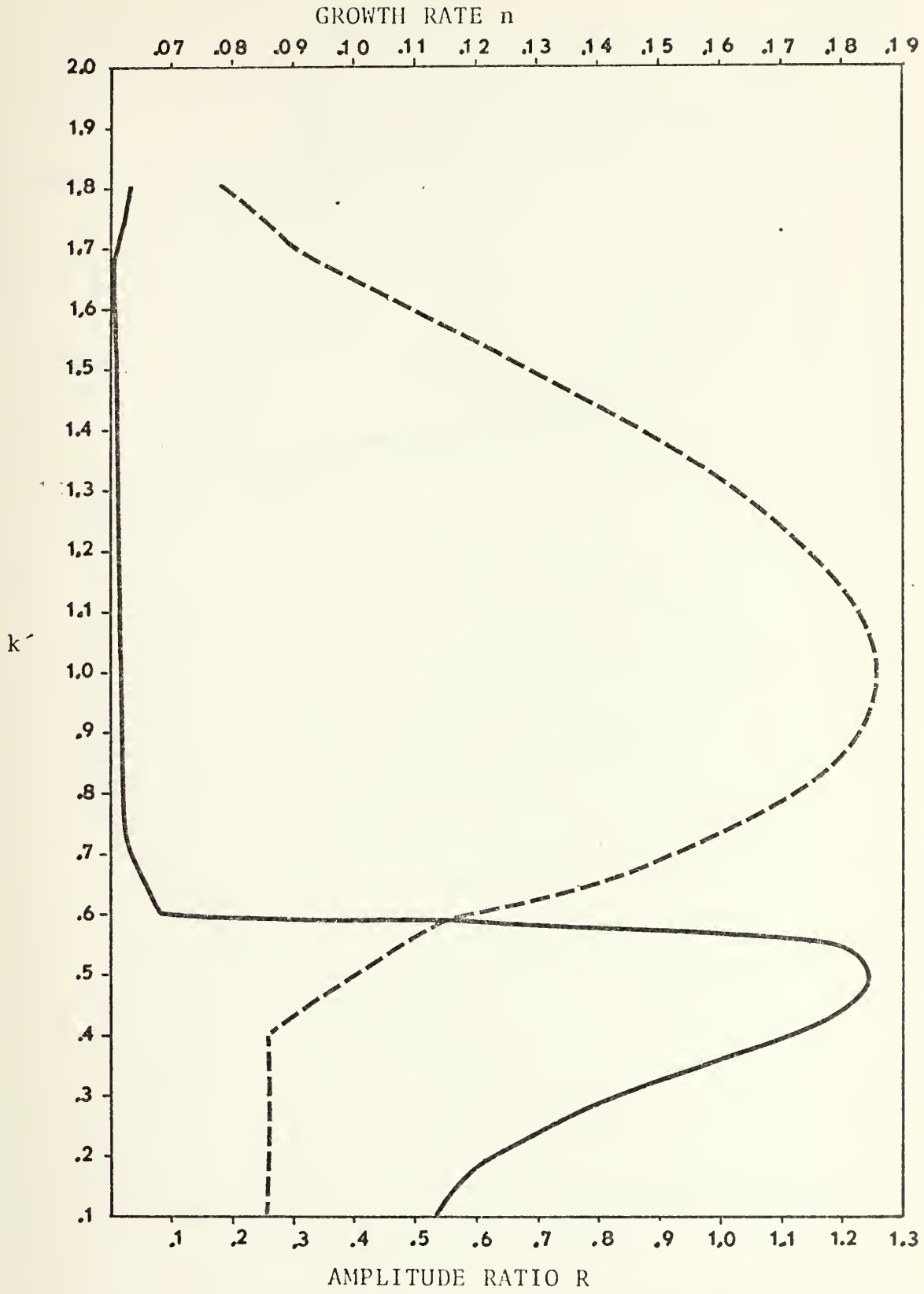

Fig. 5. Growth rate (dashed line) and amplitude ratio (solid line) as a function of wave number for experiment 3.

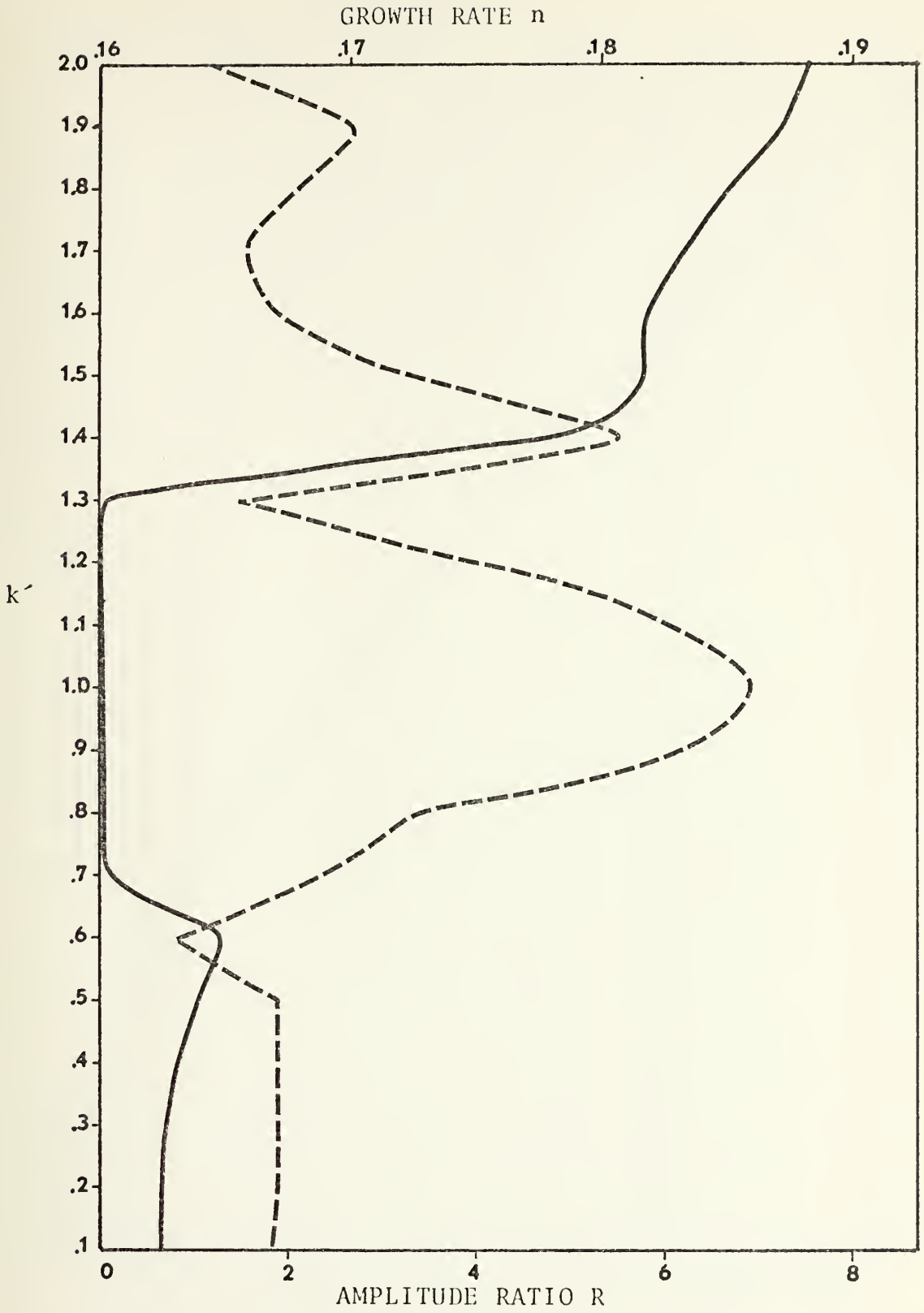

Fig. 6. Growth rate (dashed line) and amplitude ratio (solid line) as a function of wave number for experiment 4.

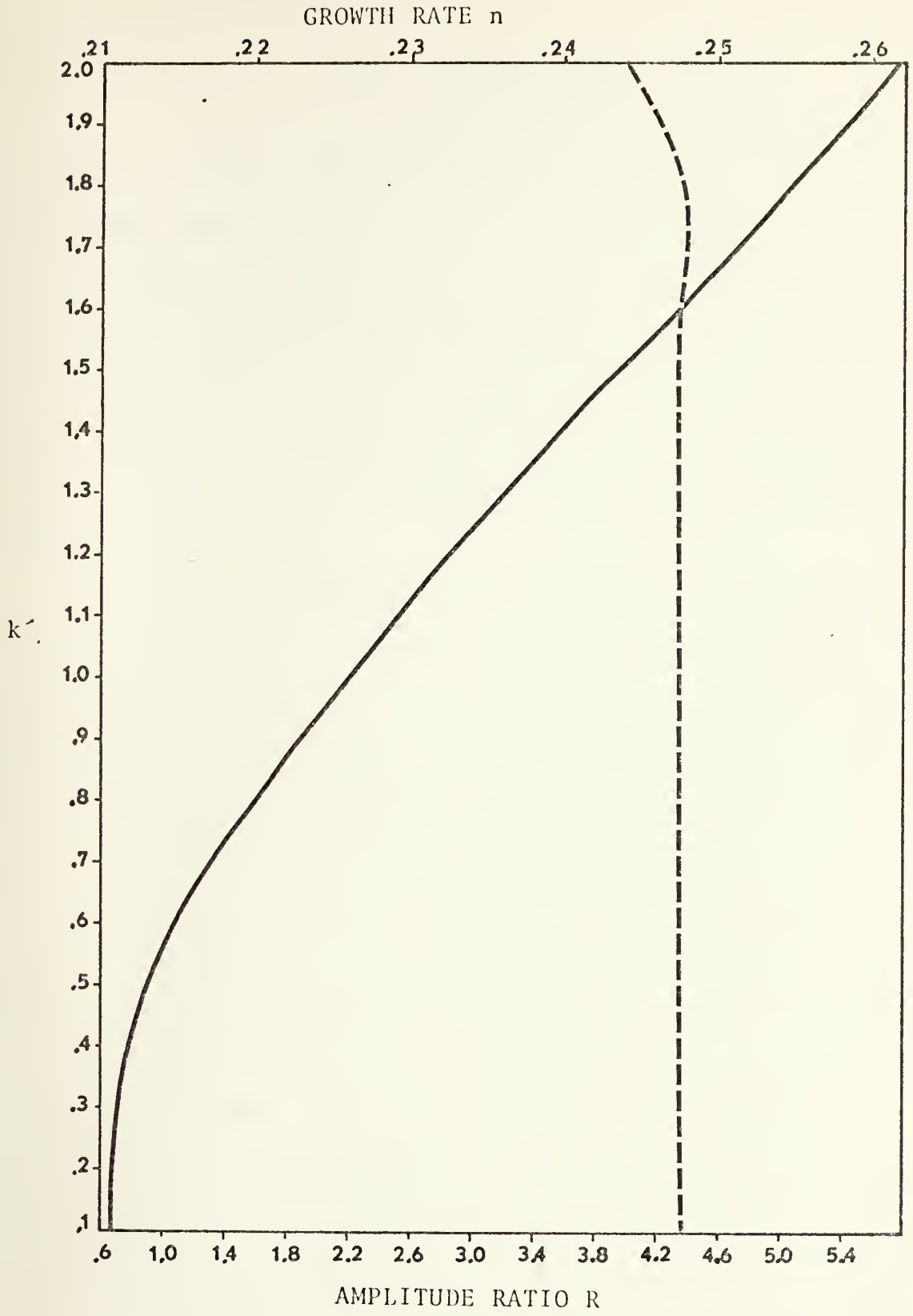

Fig. 7. Growth rate (dashed line) and amplitude ratio (solid line) as a function of wave number for experiment 5.

VIII. CONCLUSIONS

Recent studies suggest that disturbances may form through barotropic instability in the easterly jet south of the Tibetan High at 200-mb. In this thesis the instability of an analytical jet profile was investigated with a two-level quasi-geostrophic model. The downward propagation of energy from a barotropically unstable upper level disturbance was investigated to see if it could initiate lower tropospheric disturbances.

The hyperbolic secant squared wind profile was used in all of the numerical experiments. The first experiment, which contained no heating or friction, compared the growth rates with easterly and westerly flow. The easterly jet was the more unstable and its maximum growth rate was well above the growth rate for $\beta = 0$. The energy propagation was studied by introducing the jet at the upper level with no mean flow below. The ratio (R) of the disturbance amplitude at the lower level to the disturbance amplitude at the upper level was computed. With surface friction included, R decreased from high latitudes to low latitudes; at each latitude R decreased with increasing wave number. When CISK type heating was introduced with a large enough heating coefficient, the growth rate became independent of wave number. In this case R had a finite value and it increased with increasing wave number. For smaller values of the heating coefficient the

barotropic instability controls the growth rate and R remains very small.

The result that the easterly jet is more unstable than the westerly jet supports the view that barotropic instability occurs south of the Tibetan High. The small value of the amplitude ratio at low latitudes agrees with Charney's [1963] conclusion that the vertical energy propagation is small. The inclusion of CISK heating did increase the low level amplitude, but this could not occur unless a finite amplitude were present at the lower level. Since these results were obtained with a quasi-geostrophic model with only two levels, it is important to carry out further studies using more levels and also allowing for gravity waves. This would require a multi-level primitive equation model in either spherical coordinates or on an equatorial β-plane. A more sophisticated heating parameterization, such as that by Arakawa and Schubert [1974], should be used.

LIST OF REFERENCES

1. Arakawa, Akio and Schubert, Wayne H., 1974: Interaction of a cumulus cloud ensemble with the large-scale environment, part I, Journal of the Atmospheric Sciences, Vol. 31, 674-701.

2. Bates, J. R., 1970: Dynamics of disturbances on the intertropical convergence zone. Quarterly Journal of the Royal Meteorological Society, Vol. 96, 677-701.

3. Chang, Chih-Pei, 1973: On the depth of the equatorial planetary boundary layer. Journal of the Atmospheric Sciences, Vol. 30. 436-443.

4. Charney, J. G., 1963: A note on large scale motions in the tropics. Journal of the Atmospheric Sciences, Vol. 20, 607-609.

5. Charney, J. G., 1969: A further note on large-scale motions in the tropics. Journal of the Atmospheric Sciences, Vol. 26, 182-185.

6. Charney, J. G. and Eliassen, Arnt, 1949: A numerical method for predicting the perturbations of the middle-latitude westerlies. Tellus, Vol. 1, 38-54.

7. Charney, J. G. and Eliassen, Arnt, 1964: On the growth of the hurricane depression. Journal of the Atmospheric Sciences, Vol. 21, 68-75.

8. Greenspan, H. P., The theory of rotating fluids, p. 7, Cambridge University Press, England, 1968.

9. Holton, James R., Wallace, John M., and Young, J. A., 1971: Boundary layer dynamics and the ITCZ. Journal of the Atmospheric Sciences, Vol. 28, 55-64.

10. Kanamitsu, M., Krishnamurti, T. N., and Depradine, C., 1972: On scale interactions in the tropics during northern summer. Journal of the Atmospheric Sciences, Vol. 29, 698-706.

11. Kuo, Hsiano-Lan, 1949: Dynamic Instability of two-dimensional non-divergent flow in a barotropic atmosphere. Journal of Meteorology, Vol. 6, 105-122.

12. Kuo, Hsiano-Lan, 1965: On formation and intensification of tropical cyclones through latent heat release by cumulus convection. Journal of the Atmospheric Sciences, Vol. 22, 40-63.

13. Krishnamurti, T. N., 1970: 200-mb field, June, July, August 1967. Rept. No. 70-2, Dept. of Meteorology, Florida State University, Tallahassee.

14. Krishnamurti, T. N., 1971: Observational study of the tropical upper troposphere motion field during the northern hemisphere summer. Journal of Applied Meteorology, Vol. 10, 1066-1096.

15. Lipps, Frank B., 1962: Barotropic stability of the mean winds in the atmosphere. Journal of Fluid Mechanics, Vol. 12, 397-407.

16. Matsuno, Taroh, 1966: Quasi-geostrophic motions in the equatorial area. Journal of the Meteorological Society of Japan, Vol. 44, 25-43.

17. Ogura, Y., 1964: Frictionally controlled, thermally driven circulations in a circular vortex with application to tropical cyclones. Journal of the Atmospheric Sciences, Vol. 21, 610-621.

18. Ooyama, K., 1964: A dynamical model for the study of tropical cyclone development. Geofisica Internacional, Vol. 4, 187-198.

19. Richtmyer, R. D., 1957: Difference methods for initial value problems, Interscience Publishers, Inc., New York. 238 pp.

20. Robertson, Terry G., 1973: Stability of a tropical model including shear, surface friction and CISK heating. M.S. Thesis, Naval Postgraduate School, Monterey.

21. Williams, R. T. and Robertson, T. G., 1973: Effect of horizontal wind shear on CISK. Paper presented at the AGU fall annual meeting, San Francisco. (Abstract: Trans. Amer. Geophys. Union, Vol. 54, 1093.)

22. Williams, R. T., Schminke, T. K., and Newman, R. L., 1971: Effect of surface friction on the structure of barotropically unstable tropical disturbances. Monthly Weather Review, Vol. 99, 778-785.

23. Yamasaki, Masanori, 1969: Large-scale disturbances in the conditionally unstable atmosphere on low latitudes. Papers in Meteorology and Geophysics, Vol. 20, 289-336.

24. Yamasaki, Masanori, and Wada, M., 1972: Vertical structure of the barotropic unstable wave in a tropical easterly current. Journal of the Meteorological Society of Japan, Vol. 50, 271-283.

25. Yanai, Michio and Nitta, Tsuyoshi, 1968a: Finite difference approximations for the barotropic instability problem. Journal of the Meteorological Society of Japan, Vol. 46, 389-403.

INITIAL DISTRIBUTION LIST

		No. Copies
1.	Defense Documentation Center Cameron Station Alexandria, Virginia 22314	2
2.	Library, Code 0212 Naval Postgraduate School Monterey, California 93940	2
3.	Dr. R. T. Williams, Code 51Wu Department of Meteorology Naval Postgraduate School Monterey, California 93940	5
4.	Professor N. A. Phillips National Meteorological Center/NOAA World Weather Building Washington, D.C. 20233	1
5.	Officer in Charge Environmental Prediction Research Facility Naval Postgraduate School Monterey, California 93940	1
6.	Commanding Officer Fleet Numerical Weather Central Naval Postgraduate School Monterey, California 93940	1
7.	LCDR R. Hartinger 1111 Via Valle Vista Escondido, California 92025	1
8.	Dr. M. Yanai Department of Meteorology University of California Los Angeles, California 90024	1
9.	Dr. J. Young Department of Meteorology University of Wisconsin Madison, Wisconsin 53706	1
10.	Dr. R. Alexander The RAND Corporation 1700 Main Street Santa Monica, California 90406	1

11. Dr. A. Arakawa — 1
Department of Meteorology
University of California
Los Angeles, California 90024

12. Dr. C. P. Chang, Code 51Cj — 1
Department of Meteorology
Naval Postgraduate School
Monterey, California 93940

13. Professor J. G. Charney — 1
54-1424
Massachusetts Institute of Technology
Cambridge, Massachusetts 02139

14. Dr. C. Comstock, Code 53Zk — 1
Department of Mathematics
Naval Postgraduate School
Monterey, California 93940

15. Dr. R. L. Elsberry, Code 51Es — 1
Department of Meteorology
Naval Postgraduate School
Monterey, California 93940

16. Dr. J. Smagorinsky, Director — 1
Geophysical Fluid Dynamics Laboratory
Princeton University
Princeton, New Jersey 08540

17. Dr. R. L. Haney, Code 51Hy — 1
Department of Meteorology
Naval Postgraduate School
Monterey, California 93940

18. Dr. J. Holton — 1
Department of Atmospheric Sciences
University of Washington
Seattle, Washington 98105

19. Dr. Joanne Simpson — 1
Department of Environmental Sciences
2015 Ivy Road
Charlottesville, Virginia 22903

20. Dr. S. Piacsek — 1
Code 7750
Naval Research Laboratory
Washington, D.C. 20390

21. Dr. E. N. Lorenz — 1
Department of Meteorology
Massachusetts Institute of Technology
Cambridge, Massachusetts 02139

22. Dr. J. D. Mahlman — 1
Geophysical Fluid Dynamics Laboratory
Princeton University
Princeton, New Jersey 08540

23. Meteorology Library (Code 51) — 1
Naval Postgraduate School
Monterey, California 93940

24. National Center for Atmospheric Research — 1
Box 1470
Boulder, Colorado 80302

Thesis
H2955
c.1 Hartinger
Upper level baro-
tropic instability in
the tropics.